Vertical partitioning and controlling factors of gradient-based soil carbon dioxide fluxes in two contrasted soil profiles along a loamy hillslope.

Authors : Wiaux, F. [†*], Vanclooster, M. [†], Van Oost, K.[‡**]

† Environmental Sciences, Earth & Life Institute, Universitécatholique de Louvain, Croix du Sud 2, 1348 Louvain-la-Neuve, Belgium; ‡ George Lemaître Centre for Earth and Climate Research, Earth & Life Institute, Université Catholique de Louvain, Place Louis Pasteur 3, 1348 Louvain-la-Neuve, Belgium ; ** Fonds National pour la Recherche Scientifique (FNRS), Belgique.

Authors email addresses:

francois.wiaux@uclouvain.be, marnik.vanclooster@uclouvain.be, kristof.vanoost@uclouvain.be.

* Corresponding author:

E-mail address: francois.wiaux@uclouvain.be;

Phone number: 0032(0)10473712

Full postal address: Earth& Life Institute, Université catholique de Louvain, Croix du Sud n°2, BP L7.05.02, 1348, Louvain-la-Neuve, Belgium

Key words: C dynamic model; CO_2 flux; physical control; vertical partitioning; OC storage; Hillslope; cropland; loess soil.

Type of paper: Regular research paper

Abstract

We assessed soil CO_2 fluxes throughout two contrasted soil profiles along a hillslope in the central loess belt of Belgium. First, we measured time-series of soil temperature, soil moisture and CO_2 concentration at different depths in the soil profiles for two periods of 6 months. Subsequently we calculated the CO_2 flux at different depths, using Fick's diffusion law and horizon specific diffusivity coefficients. The soil diffusivity coefficients were calibrated using profile specific surface CO_2 flux chamber measurements. The calculated fluxes allowed assessing the contribution of different soil layers to surface CO_2 fluxes and elucidating deep soil controlling factors on CO_2 emission.

The results show that approximately 90 to 95 % of the surface CO2 fluxes originate from the first 10 centimeters of the soil profile at the footslope. This indicates that soil OC at such a footslope can be stored along the main part of the soil profile (below 10 cm) and submitted to a long-term stabilization. We also observe that time-series of soil CO_2 emissions at the summit are in accordance with the temporal dynamics of temperature. In contrast, at the footslope, we highlight that long periods of CO_2 accumulation alternate with peaks of important surface release due to the high water filled pore space that limits the transfer of CO_2 along the soil profile at this slope position.

1. Introduction

Soils play a major role in the global C budget, as they contain 2 to 3 times more C than the atmosphere (Eswaran et al., 1993; Lal et al., 2003). There is now significant concern about the contribution of soil OC to future climate change where a climate change driven acceleration of soil OC decomposition could represent a positive feedback on climate. In addition to the role of soil mineralogy and microbial communities, recent studies highlight the importance of soil bio-physical conditions that may vary substantially with time and across landscapes (e.g. Dai et al., 2012). In addition to the combined effects of soil moisture, temperature and OC quality on soil microbial activity (e.g. Wiaux et al., 2014b), recent studies show the importance of physical controls on CO_2 fluxes such as gas diffusion barriers along soil profiles .(e.g. Ball, 2013; Maier et al., 2011). Furthermore, most process studies so far have focused on the soil surface layer while there is now increasing awareness that subsoil OC represents an important C store that interacts with the atmosphere (Rumpel and Kögel-Knabner, 2011). Recent studies (Rumpel and Kögel-Knabner, 2011) highlighted that deep soil OC is highly processed, and showed the need to consider C fluxes originating from deeper soil horizons. This is particularly relevant in landscapes with complex topography where buried OC in depositional areas contributes substantially to soil C emissions (e.g. Van Oost et al., 2012; Wang et al., 2014 and Wiaux et al., 2014a). Goffin et al. (2014) showed that the upper first 30 centimeters of a forest soil profile contribute substantially to the total surface CO_2 flux. However, to our knowledge, a vertical partitioning has not been evaluated in agro-ecosystems or in systems with contrasting soil physical and/or chemical properties.

In this study, we aim to elucidate the role of physical controls on soil-atmosphere CO_2 fluxes and its variation with soil depth. To that aim, we present a comparative analysis between two contrasting soil profiles along an eroded and cultivated hillslope. The objectives of this study are: (i) to quantify the relative contribution of soil surface and subsoil OC to CO_2 fluxes through a vertical partitioning of these fluxes; and (ii) to identify the role of soil physical properties using time-series of soil moisture measurements and gas diffusivity at different depths. The selected study site is characterized by two contrasting soils in terms of soil hydrological regimes and structure.

65 # 2. Material and methods

66 ## 2.1. Study site description

67 The study was carried out in the Belgian loam belt along a cultivated hillslope of 150 meters length
68 (50.6669°N, 4.6331° W). The site has a maritime temperate climate, with an average annual
69 temperature of 9.7°C and an average annual precipitation of 805 mm. The slope percentage in the
70 backslope area ranges between 8.5 and 16%, with a mean slope of 12%. The slope percentage in the
71 convex shoulder area ranges between 4 to 8.5%, with an average of 6%. The field was plowed (0-30
72 cm soil surface layer) every year. Each year, manure and nitrate fertilization was carried out. The
73 previous crop rotation was winter wheat, maize and spring wheat. The study site has been described in
74 detail in Wiaux et al. (2014a,b). For this study, we selected two measurement stations along the
75 hillslope: one at the summit and one at the footslope position. The soil is a Dystric Luvisol type at the
76 summit and a Colluvic Regosol in the depositional area at the footslope (Wiaux et al., 2014a,b). The
77 soil properties of these two soil profiles have been characterized by Wiaux et al. (2014a,b): soil total
78 OC, labile OC and porosity profiles are illustrated in Fig. 1 and 2, respectively.

79 We measured the total porosity (ϕ)in the laboratory by weighing 100 cm^3 undisturbed soil cores both
80 at saturation and after oven drying at 105°C for 48h. We deduced ϕ from the mass of water needed to
81 fill sample pores. We calculated the air-filled porosity (ε) as the difference between ϕ and volumetric
82 water content (VWC). We calculated average and standard deviation values on triplicate samples for
83 each depth.

84 We characterized soil water retention (SWR) curves using undisturbed soil cores at 10, 25, 35, 50, 70
85 and 95 cm depth, with 3 replicates at each depth. We obtained the ε_{100} and b parameters of the
86 Campbell (1974) SWR model by fitting the model to the SWR observations (Moldrup et al. 2000).

87 ## 2.2. Monitoring of soil CO_2, water and temperature

88 We measured soil CO_2 concentrations using purpose-built soil CO_2 probes. The CO_2 sensor in the
89 probe is based on the CARBOCAP® Single-Beam Dual Wavelength non-dispersive infra-red (NDIR)

technology (GMM221, Vaisala corp., Vantaa, Finland). The analytical precision is 1.5% of the measurement range added to 2% of the observed value. The sampling head of the CO_2 probe is a cylinder of 18.5 mm diameter and 40 mm long, covered with a PTFE (polytetrafluoroethylene) membrane, enabling gas exchange and protection against water infiltration. Since the GMM221 sensors were not designed for wet soil conditions, the sensors were encapsulated into an additional perforated PVC tube, providing an additional protection against water (Fig. 1). This tubing method is an adaptation of the technique presented by Young et al. (2009). We inserted these tubes vertically into the soil, after creating bore holes with a diameter that equals the diameter of the PVC tubes. This approach avoids the need to backfill the bore hole, which will disturb the soil structure and diffusion process. Two rubber stoppers, one at 155 mm from the tube head, and another at the top of the tube, prevented atmospheric air from penetrating into the gas sampling volume. Petroleum jelly on these two rubber stoppers ensured a perfect air- and water-tightness and we verified this under laboratory conditions before using the probes. We used a nylon membrane to avoid soil particles entering the perforated tube and to limit further water infiltration.

We monitored soil temperature using a thermistor probe (Therm107, Campbell Scientific Lt., UK). Analytical precision is 0.4°C. We monitored soil volumetric water content (VWC) using Time Domain Reflectrometry (TDR) probes. We used Topp's equation (Topp et al., 1980) to determine VWC from the measured apparent dielectric constant measured. We used the parameters of the Topp's equation as identified by Beff et al. (2013). In this study latter study, the Topp's equation was calibrated for an experimental field in the close vicinity of our study site, using the method of Heimovaara (1993) and following the protocol described by Garré et al. (2008). We recorded water, temperature and CO_2 concentration profiles measurements with an automatic data logger (CR1000, Campbell Scientific Lt., UK), connected to a multiplexer (AM16/32, Campbell Scientific, Campbell Scientific Lt., UK).

In order to obtain an equilibrated soil environment around the soil VWC, temperature and CO_2 probes, we started measurements 1 month after the installation of the probes. We covered the measurement

plots with a synthetic permeable geotextile during the complete measurement period. This avoided vegetation growth and any autotrophic contribution to the soil respiration.

The sampling design is depicted in Fig. 4. At each of the 2 slope positions, we measured soil VWC and CO_2 concentrations profiles with 3 replicates on each measurement depth (Fig. 4). We collected 18 VWC profiles (6 soil depths, 3 replicates), at each of the 2 slope positions. We measured VWC at a depth of 10, 25, 35, 50, 70 and 95 cm depths (Fig. 4). We measured the temperature at 4 soil depths (10, 25, 45, 85 cm) without replicates (Fig. 4). We measured CO_2 concentrations at a depth of 10, 25, 45 and 85 cm. We also performed surface CO_2 fluxes measurements with an infra-red gas analyzer (IRGA) linked to a survey chamber at 16 dates (profile and surface sampling time was within a 30 minutes time interval). Note that the averaged values of CO_2 concentration for each observation depth cover the same area as the IRGA chamber network located at the soil surface (Fig. 4). These reference surface CO_2 fluxes allowed calibrating parameters of the soil gas diffusion model, ensuring the accuracy of profile CO_2 fluxes (section 2.3).

We adjusted the concentration ranges of the CO_2 probe for each soil depth and for each slope position. This allowed an optimal fit of the probes to the local concentrations. Each probe has to characterize the entire range of values encountered during the seasons while at the same time, it should have a sufficiently narrow measurement range to ensure measurement precision At the summit position, measurements ranged between 0-2 % at 12, 25, 45 cm depth and between 0-5 % at 85 cm depth. At the footslope position, measurements ranged between 0-5 % at 12 cm depth, between 0-10 % at 25 and 45 cm depth and between 0-20 % at 85 cm depth.

We recorded hourly time-series of VWC, temperature and CO_2 concentrations from 12 May to 13 December 2012 and from 14 May to 22 November 2013 at the footslope position and from the 2 June to 13 December 2012 and from the 14 June to 22 November 2013 at the summit position. In 2012, important parts of CO_2 measurements were not recorded as a result of sensors failures and/or the use of an unsuitable initial measurement range of some sensors.

To increase the quality of the soil concentration data time-series, we removed observations where the battery voltage was lower than 11.5 V. We also corrected soil profile CO_2 concentrations measurements for temperature variations using the empirical formulas described by Tang et al. (2003). This allowed removing the impact of temperature on the CO_2 reading of the CO_2 probe, since the CARBOCAP® technology is temperature dependent. The probe manufacturer (Vaisala corp., Vantaa, Finland) provided probe specific parameters values for the correction formulas.

We averaged triplicate VWC and CO_2 concentrations data, providing an average value for each soil depth and slope position. Note that averaging strategy allows to account for the spatial variability of VWC and CO_2 concentrations (Maier and Schack-Kirchner, 2014), by extending the measurement footprint to an area of c. 5 m^2.

We calculated soil temperature and VWC profiles using a linear interpolation between the depth specific values within the profile. We kept the values constant between the sampling point at the top of the profile and the soil surface. We calculated the CO_2 concentrations profiles by fitting Eq. 2 to the observations. We evaluated the performance of this fitting by means of the regression coefficient (R^2). When the R^2 values were lower than a threshold value of 95%, we considered the CO_2concentration profile as unreliable and we did not retain the resulting CO_2 fluxes in final analysis.

2.3. Calculation of the CO_2 fluxes

We calculated the CO_2 flux using Fick's first law of diffusion according to the gradient method (Eq. 1, e.g. Maier and Schack-Kirchner, 2014):

$$F_{CO_2} = -D_s \frac{\partial CO_2}{\partial z} \quad \text{(Eq. 1)}$$

where F_{CO_2} is the soil CO_2 flux [µmol m^{-2} s^{-1}], D_s the diffusivity of CO_2 in soil [m^2 s^{-1}], CO_2 the soil CO_2 concentration [µmol m^{-3}], and $\frac{\partial CO_2}{\partial z}$ the vertical soil CO_2 gradient.

In order to calculate the vertical soil CO_2 gradient, we used a double sigmoidal equation (Eq. 2), which allows accounting for some curve concavity variations (Maier and Schack-Kirchner, 2014):

$$CO_2(z) = 0.04 + A\left(\left(\frac{1}{1+e^{-\gamma_1 z}}\right) + \left(\frac{1}{1+e^{-\gamma_2 (z-d)}}\right) - \left(\frac{1}{2} + \frac{1}{e^{\gamma_2 d}+1}\right)\right) \quad \text{(Eq. 2)}$$

where z is the soil depth [cm], d is the soil depth [cm] at which the sharpness of the curve changes due to a diffusion barrier, $\gamma_1$and γ_2 [cm^{-1}] are fitted parameters which characterize the sharpness of the curve, respectively above and below the soil depth d, and A [%] is a reference value used to define the fitted asymptotic value of the CO_2 concentration at infinite depth. We fitted the A, d, $\gamma_1$and γ_2 parameters for each CO_2-profile using the trust-region-reflective optimization algorithm in Matlab ©. The derivative of Eq. 2 provided the CO2 gradient ($\frac{\partial CO_2}{\partial z}$) used in Eq. 1.

The diffusivity of CO_2 in soil, D_s (Eq. 1) is a function of the diffusivity of CO_2 in free air (varying with temperature T and pressure, e.g. Davidson *et al*., 2006) and of the gas tortuosity factor (ξ) (Eq. 3):

$$D_s = \xi\, 1.47\, 10^{-5} \left(\frac{T+273}{273}\right)^{1.75} \quad \text{(Eq. 3)}$$

where ξ depends on soil physical and hydrological properties. We used the Moldrup *et al*. (2000) model (Eq. 4) which was shown to provide the most accurate and precise results (Davidson et al., 2006; Goffin et al., 2014);

$$\xi = (2{\varepsilon_{100}}^3 + 0.04\varepsilon_{100}) \left(\frac{\varepsilon}{\varepsilon_{100}}\right)^{2+3/b} \quad \text{(Eq. 4)}$$

where ξ is the gas tortuosity factor, ε [$m^3\ m^{-3}$] is the soil air-filled porosity, b [-] is the slope of the Campbell (1974) soil water retention curve model between -100 and -500 cm H_2O water suction, and ε_{100} [$m^3\ m^{-3}$] is the soil air-filled porosity at a soil water potential of -100 cm H_2O.

CO_2 fluxes, as assessed by the gradient based method, were calculated on an hourly time-scale, and then integrated on a daily basis. Temperature, VWC, diffusivity and CO_2 concentration values were also averaged on a daily basis.

In contrast to other studies (e.g. Pingintha et al., 2010; Turcu et al., 2005), we did not aggregate the soil diffusivity coefficient for the entire soil profile or for an entire soil layer. We considered the

187 vertical distribution explicitly, and integrated Eq. 4 in the finite difference numerical solution of Eq.
188 1. In this numerical integration, we used a depth increment of 0.1cm and constrained the surface CO_2
189 concentrations with atmospheric CO_2 levels (i.e. 400 ppm).

190 We calibrated the diffusion model by adjusting the parameters related to the gas diffusion coefficient
191 (i.e. b and ε_{100}) such that calculated fluxes fit punctual CO_2 fluxes observations at 16 dates spread
192 along the measurement period. We obtained these observations by means of a portable infra-red gas
193 analyzer with an automated closed dynamic chamber (LI-8100A system, LI-COR, United-States),
194 following Davidson et al. (2002). The sampling design of these surface chamber CO_2 fluxes
195 measurements on the same study site has been described in Wiaux et al. (2014 b). Comparing the
196 gradient-based CO_2 fluxes with directly measured IRGA CO_2 fluxes, we obtained a good prediction
197 with a R2 of 92% for all soil types together. This ensures the consistency (and consequently the
198 precision) of the calculated fluxes. The slope of the fit (i.e. 1.05 and 1.22, respectively in 2012 and
199 2013) was used to correct the calculated fluxes and to ensure the accuracy.

200 ## 2.4. Vertical partitioning of CO_2 fluxes

201 We partitioned the continuous CO_2 flux profiles obtained using Eq.2 into 10 slides of 10 centimeters
202 along the soil profile. For each soil slide, we calculated the difference between the top and bottom
203 fluxes. We divided this difference by the total CO_2 flux (e.g. the value at the soil surface). This
204 provides the relative contribution in terms of both CO_2 production and transfer (in %) of each soil slide
205 to the surface CO_2 flux (e.g. Goffin et al., 2014; Maier and Schack-Kirchner, 2014).

206 In order to allow an easy representation of the temporal dynamic of this vertical partitioning, we
207 averaged values on a semi-seasonal time-scale. Standard deviation values reflect the variability over
208 time during each semi-season.

3. Results

3.1. Spatio-temporal analysis of measured soil variables

Fig. 5 shows the spatio-temporal variation of soil temperature and moisture, while Fig. 6 shows the spatio-temporal variation of CO_2 fluxes, concentrations and diffusion. All these values correspond to in-situ measurements during a 6 month period in 2013. Similar measurements have been carried out in 2012 and display similar spatio-temporal trends (data not shown).

During the observation period, the soil temperature (Fig. 5A) did not significantly differ between the summit and the footslope, although higher temperatures were observed at the summit profile for some shorter periods (e.g. day of year 180 to 220 where temperatures are approximately 2 to 3 °C higher). The mean daily surface temperatures range between 4°C to 28°C at the summit, and between 4°C to 25°C at the footslope.

The space-time dynamics of the soil volumetric water content (VWC, Fig. 5B) differ substantially between the summit and the footslope profiles. At the footslope, the observed soil VWC at different soil depths varied in a narrow range (0.36 to 0.39 cm^3 cm^{-3}). In contrast, soil VWC at the summit varied between 0.23 to 0.34 cm^3 cm^{-3} for the plow layer (0-30cm depth) and higher values (approximately 0.5 cm^3 cm^{-3}) were observed for the rest of the soil profile. The soil at the summit position was the wettest during the early spring and the late autumn and driest in the summer. At the footslope, soil VWC reached the saturation level in the early summer after an important rainfall event and then slowly decreased until the early autumn and reached saturation again in the late autumn.

In contrast to the VWC, the soil gas diffusivity (Fig. 6C) reached its maximum value in the summer at the summit while it was low at the footslope. Soil gas diffusivity was approximately 10 times lower at the footslope than at the summit.

The soil CO_2concentrations at both the summit and the footslope increased gradually from spring to late summer. Thereafter, concentrations dropped again and lowest values were observed in the late autumn. The ranges of CO_2 fluxes obtained for the footslope and summit profiles were very similar.

However, their temporal distribution was different: the periods characterized by high CO_2 fluxes did not occur at the same time and had a different duration. For all soil profiles, CO_2 fluxes decreased with depth and reached null values at approximately30 cm depth at the summit and at approximately 15 cm depth at the footslope.

3.2. Shape and variability of CO_2 concentrations and fluxes profiles

The observed soil CO_2 concentrations (Fig. 6Bb) increased with soil depth, from the atmospheric value of 0.04 % at the surface to concentrations which were two orders of magnitude higher at 100 cm depth (CO_2,(z) in Eq.2) (Fig. 6Bb). For the measurement period of 6 months considered here, CO_2 concentration values at 100 cm depth were three to four times higher at the footslope position than at the summit position. In 2013, these values ranged between 0.86 to 3.46 % at the summit position and between 3.68 to 9.12 % at the footslope position.

The observed CO_2 concentration profiles followed a double exponential trend (Eq. 2). This particular model fits our observations relatively well, with regression coefficients ranging between 97 to 100%. The second exponential curve starts approximately at the middle of the profile, and is particularly pronounced at the footslope, reflecting a shift of nearly 4% CO_2 between 44 and 100 cm depth. Standard deviations around averaged values of observed hourly CO_2 concentrations at each depth are given in Table 1. The small-scale spatial variability is low relative to the mean values of CO_2 concentrations, the only exception being the footslope at 25 cm depth where the maximum standard deviation exceeded the maximum mean value.

The CO_2 fluxes (Fig. 6A) were calculated based on both CO_2 concentrations and diffusivity. For all soil profiles, CO_2 fluxes decreased with depth and reached null values at c.30 cm depth at the summit and at c. 15 cm depth at the footslope.

3.3. Vertical partitioning of CO_2 fluxes

The distribution of the soil CO_2 fluxes in the profile is illustrated in Fig. 7. At the footslope, 90 to 95 % of the surface CO_2 fluxes were generated in the first ten centimeters of the soil profile. The soil

layer between 10 and 20 cm contributed for only 5 to 10 %, and the deeper layers did not significantly contribute to the surface fluxes. At the summit, the relative contribution of the different soil layers was more dynamic in time, with a contribution of the first ten centimeters of the soil profile ranging from 80 % at the late spring, decreasing to 60 % in the early summer, and reaching 40 % from late summer to the late autumn. At the summit, the first 30 centimeters of the soil profile significantly contributed to surface fluxes. This contribution decreased with depth in the late spring and the early summer, but is homogeneously distributed with depth for the rest of the time. At the summit, soil layers deeper than 30 cm depth sometimes contributed for up to 20% of the total flux, especially in the autumn. Between 40 to 50 cm depth, and 80 to 90 cm depth, some negative contribution (i.e. CO_2 uptake) up to -20% is also observed.

4. Discussion

4.1. Soil physical control on CO_2 emissions

The observed differences in the temporal dynamics of surface soil CO_2 fluxes between the footslope and summit soil profiles (Fig. 6A) indicates that the controlling factors are not the same. At the summit, on one hand, the dynamic of surface soil CO_2 fluxes (Fig. 6A) clearly follows the temperature variations (Fig. 5A, maximum during the summer). At the footslope, on the other hand, the soil surface CO_2 flux was small even when temperature increased and remained relatively small throughout the summer period (Fig. 6A). This is most likely related to the high VWC values observed at the footslope (Fig. 5B), as it is well known that VWC negatively impacts soil CO_2 emissions (e.g. Webster et al., 2008b; Perrin et al., 2012; Wiaux et al., 2014b). More precisely, we suggest that the factor controlling CO_2 emissions at the footslope is not only VWC but also the difference between the VWC and the water saturation level of the soil pore spaces. While the VWC at the footslope remained high throughout the year, we observed that the soil surface CO_2 flux dramatically increased when the gas diffusivity exceeded a threshold value of c. 0.1 $cm^2\ d^{-1}$ (i.e. from day 255 to 305 of year 2013, Fig. 6A). Hence, we argue that the CO_2 emissions at the footslope profile are related to the fact that a high VWC both: (i) strongly limits the transfer of biotic CO_2 along the soil profile, and (ii) reduces the

285 production of CO_2 in itself due to the lack of oxygen for the microbial community. In both cases, the
286 lower CO_2 emissions at the footslope profile relative to the summit, are due to gas diffusion limitations
287 (even indirectly in the case of oxygen lack). This is in sharp contrast to the summit profile where gas
288 can easily diffuse throughout the year and along the entire soil profile (Fig. 6C).

289 In the period preceding the important CO_2 emissions (i.e. from day 255 to 305 of year 2013, Fig. 6A),
290 the soil CO_2 cannot move along the soil profile and accumulates within soil pores. This results in a
291 CO_2 concentration increase both in the early and the late summer, especially below 50 cm depth (Fig.
292 6). This phenomenon is particularly evident below the compacted soil layer between 40 cm and 50 cm
293 depth. Based on the porosity profile illustrated in Fig. 1, this suggests that for our footlslope soil
294 profile , which is a Colluvic Regosols, gas diffusion barriers strongly impact the CO_2 concentration
295 profile, and hence the temporal dynamics of soil surface CO_2 fluxes. This is in agreement with recent
296 studies (e.g. Ball, 2013) that show that soil pore continuity and size are key to understand the
297 mechanisms regulating the soil gases emissions.

298 As a consequence, the significantly higher CO_2 concentrations observed at the footslope, especially for
299 deeper soil layers, are probably not related to the large amount of labile OC that was found at this
300 position (shown in Wiaux et al., 2014a,b), but more likely result from the accumulation of CO2 during
301 periods with a very low diffusivity. Maier et al. (2011) showed that the CO_2 efflux can deviate from
302 the instantaneous soil respiration due to CO_2 storage into soil pore spaces. Hence, we suggest that at
303 the footslope, soil physical properties are the dominant control on surface CO_2 fluxes. In summary, we
304 highlight that the mechanisms that govern soil surface CO_2 emissions are highly variable in both space
305 and time. On a well-drained soil at the summit of a hillslope, the observed soil CO_2 emissions were
306 directly related to soil microbial respiration and CO_2 production (demonstrated in Wiaux et al., 2014b).
307 However, at the footslope of the hillslope, which is characterized by a different hydrological regime,
308 we observed that the temporal dynamic of soil CO_2 emissions were more closely related to physical
309 transfer mechanisms: long periods of CO_2 production and accumulation alternate with periods of
310 important release at the soil surface.

4.2. Soil organic carbon storage in downslope deposits

The soil respiration rate can be interpreted as an indicator of soil OC persistence (e.g. Gregorich et al., 1994). However, a further analysis of what occurs along the soil profile is needed to thoroughly answer the question of the persistence of OC. The vertical partitioning of the soil CO_2 fluxes, as illustrated in Fig. 7, shows that during the observation period, 90 to 95 % of the surface CO_2 flux originated from the first ten centimeters of the soil profile at the footslope. Given the important amount of OC until up to 100 cm depth in our study site (Fig. 1, Wiaux et al., 2014 a), this observation is not in agreement with the study of Goffin et al. (2014), who suggested that the relative contribution of a soil layer to the surface CO_2 fluxes is related to OC distribution along the soil profile. However, while similarities exist in the physical controls and the method used to calculate the vertical partitioning, the study of Goffin et al. (2014) reports on CO_2 production in forest soils, preventing any direct quantitative comparison.

In addition, the substantial contribution of the upper soil layers found here was not related to higher temperatures (Fig. 5A), contrary to what was suggested by Takahashi et al. (2004). According to the CO_2 concentration and diffusivity profiles (Fig. 6C), the relative contribution of the soil layers to the surface CO_2 flux is more likely governed by soil physical controls (Ball, 2013) rather than by biological production depending on thermal energy and OC substrate. Here, soil gas diffusivity strongly decreases from 10 to 40 cm depth (where diffusivity is null) at the two slope positions, and the profile of CO_2 concentration displays no gradient between 10 and 40 cm depth, particularly at the footslope (Fig. 6A).

Here, we show that despite the fact that the footslope profiles generates CO_2 fluxes which exceed those observed at the summit position (demonstrated in Wiaux et al., 2014b), the contribution of soil layers below 10 cm depth is very small (Fig. 7). The OC in the top layer of the soil profile (i.e.0-10 cm) contributed for c. 90% of the total CO_2 flux at the footslope position (Fig. 7). This can be explained by environmental conditions specific to this 0-10 cm layer playing in favor of both microbial respiration and gas diffusion. There are no limitations related to both diffusion barriers and

337 access to the oxygen disappear close to the soil surface. Hence, the only impact of soil VWC on soil
338 respiration is its positive effect as it provides a more easy access for soil micro-organisms to their OC
339 substrate, and to the enhancement of their metabolic activities by water (Akinremi et al., 1999;
340 Castellano et al., 2011; Herbst et al., 2008; Howard and Howard, 1993; Šimůnek and Suarez, 1993).
341 The combination of this high amount and high quality of soil OC (Fig. 1, as described by Wiaux et al.,
342 2014a) with this net positive effect of soil VWC results in a strong increase of microbial respiration
343 rates.

344 Finally, our results suggest that buried soil OC in colluvial deposits is effectively protected from
345 mineralization below 10 cm depth, which corroborates the assumption of a long-term stabilization of
346 buried OC in colluvial soils as suggested in the literature (e.g. Doetterl et al., 2012; Berhe et al., 2008,
347 2012a).

348 # 5. Conclusion

349 In this study, we evaluated the factors controlling soil carbon dioxide fluxes for two soil profiles along
350 a hillslope characterized by contrasting physical and chemical characteristics. At the summit position
351 of the studied hillslope, the time course of surface soil CO_2 fluxes was strongly related to soil
352 temperature and maximum CO2 fluxes were observed during the summer. Here, the observed soil CO_2
353 emissions are directly related to soil micro-organisms respiration and associated biotic CO_2
354 production. In contrast, the higher levels of water filled pore space observed at the footslope profiles,
355 strongly limited the transfer of biotic CO_2 throughout the soil profile. Here, the soil surface CO_2 flux
356 substantially increased for limited amounts of time when the gas diffusivity exceeded a threshold
357 value. As a result, the time course of observed soil CO_2 emissions was to a large extent explained by
358 physical transfer mechanisms: long periods of accumulation alternate with shorter periods of important
359 CO_2 release. The vertical partitioning of the soil CO_2 fluxes for the footslope profiles showed that,
360 during the observation period, 90 to 95 % of the surface CO_2 fluxes originated from the first 10
361 centimeters of the soil profile. This study highlights the need to include soil physical properties and
362 their dynamics directly into soil OC models.

Author contribution

F.W. designed the experiments, and carried out the research. M.V., K.V.O. and F.W. analyzed the results. F.W. wrote the main part of the paper and prepared the manuscript with contributions from all co-authors.

Acknowledgement

This study was funded by the Fonds National pour la Recherche Scientifique (FNRS, Belgium, convention n° 1.A306.12) and by the Fonds de la Recherche Fondamentale Collective (FRFC, convention n° 2.4590.12). F.W. and K.V.O. are supported by the FNRS. We thank the technician team of the UCL, especially F. Laurent for its precious help and ideas in establishing the experimental setup for in-situ soil CO_2 concentration profile measurements, and S. François for having achieved most of field campaigns of soil surface respiration measurements during more than 2 years. We kindly acknowledge Dr. J. Gillabel, from the Katholiek Universiteit van Leuven (Belgium), for its precious scientific and technical advices. The experimental design illsutrated on Fig. 4 has been inspired from which described in his PhD thesis (non peer-reviewed works).

References

Akinremi, O., McGinn, S., McLean, H., 1999.Effects of soil temperature and moisture on soil respiration in barley and fallow plots. Canadian Journal of Soil Science 79, 5-13.

Ball, B.C., 2013. Soil structure and greenhouse gas emissions: A synthesis of 20 years of experimentation. European Journal of Soil Science 64, 357-373.

Beff, L., Günther, T., Vandoorne, B., Couvreur, V., Javaux, M. (2013). Three-dimensional monitoring of soil water content in a maize field using Electrical Resistivity Tomography. Hydrology and Earth System Sciences17, 595-609.

Berhe, A.A., Harden, J.W., Torn, M.S., Harte, J., 2008. Linking soil organic matter dynamics and erosion-induced terrestrial carbon sequestration at different landform positions. J. Geophys. Res. 113, G04039.

Berhe, A.A., Harden, J.W., Torn, M.S., Kleber, M., Burton, S.D., Harte, J., 2012.Persistence of soil organic matter in eroding versus depositional landform positions. J. Geophys. Res. 117, G02019.

Berhe, A.A., Kleber, M., 2013. Erosion, deposition, and the persistence of soil organic matter: Mechanistic considerations and problems with terminology. Earth Surface Processes and Landforms 38, 908-912.

CAMPBELL, G.S., 1974. A Simple Method for Determining Unsaturated Conductivity From Moisture Retention Data. Soil Science 117, 311-314.

Castellano, M.J., Schmidt, J.P., Kaye, J.P., Walker, C., Graham, C.B., Lin, H., Dell, C., 2011. Hydrological controls on heterotrophic soil respiration across an agricultural landscape. Geoderma 162, 273-280.

Chaopricha, N.T., Marín-Spiotta, E., 2014. Soil burial contributes to deep soil organic carbon storage. Soil Biology and Biochemistry 69, 251-264.

Dai, Z., Trettin, C.C., Li, C., Li, H., Sun, G., Amatya, D.M., 2012. Effect of assessment scale on spatial and temporal variations in CH 4, CO 2, and N 2O fluxes in a forested Wetland. Water, Air, and Soil Pollution 223, 253-265.

Davidson, E.A., Savage, K., Verchot, L.V., Navarro, R., 2002. Minimizing artifacts and biases in chamber-based measurements of soil respiration. Agricultural and Forest Meteorology 113, 21-37.

Davidson, E.A., Savage, K.E., Trumbore, S.E., Borken, W., 2006. Vertical partitioning of CO_2 production within a temperate forest soil. Global Change Biology 12, 944-956.

Doetterl, S., Six, J., Van Wesemael, B., Van Oost, K., 2012. Carbon cycling in eroding landscapes: Geomorphic controls on soil organic C pool composition and C stabilization. Global Change Biology 18, 2218-2232.

Epron, D., Bosc, A., Bonal, D., Freycon, V., 2006. Spatial variation of soil respiration across a topographic gradient in a tropical rain forest in French Guiana. Journal of Tropical Ecology 22, 565-574.

Eswaran, H., Van Den Berg, E., Reich, P., 1993. Organic carbon in soils of the World. Soil Science Society of America Journal 57, 192-194.

Eugster, W., et al., 2010. Management effects on European cropland respiration. Agriculture, Ecosystems & Environment 139, 346-362.

Gallagher, M., Doherty, J., 2007. Parameter estimation and uncertainty analysis for a watershed model. Environmental Modelling & Software 22, 1000-1020.

Garr´e, S., Huisman, S., andWeihermüller, L.: Manual for TDR calibration, Agrosphere Institute, ICG IV, ForschungszentrumJülichGmbH, 52425 Jülich, Germany, 1–18, 2008.

Goffin, S., Aubinet, M., Maier, M., Plain, C., Schack-Kirchner, H., Longdoz, B., 2014. Characterization of the soil CO2 production and its carbon isotope composition in forest soil layers using the flux-gradient approach. Agricultural and Forest Meteorology 188, 45-57.

Gregorich, E.G., Carter, M.R., Angers, D.A., Monreal, C.M., Ellert, B.H., 1994.Towards a minimum data set to assess soil organic matter quality in agricultural soils. Canadian Journal of Soil Science 74, 367-385.

Heimovaara, T. J.(1993). Design of triple-wire time domain reflectometry probes in practice and theory, Soil Sci. Soc. Am. J 57, 1410–1417.

Herbst, M., Hellebrand, H.J., Bauer, J., Huisman, J.A., Simunek, J., Weihermuller, L., Graf, A., Vanderborght, J., Vereecken, H., 2008. Multiyear heterotrophic soil respiration: Evaluation of a coupled CO2 transport and carbon turnover model. Ecological Modelling 214, 271-283.

Houghton, R.A. (2003). Why are estimates of the terrestrial carbon balance so different? Global Change Biology 9, 500-509.

Howard, D.M., Howard, P.J.A., 1993. Relationships between co2 evolution, moisture content and temperature for a range of soil types.Soil Biology and Biochemistry 25, 1537- 1546.

IPCC, 1990.Detection of the greenhouse effect in the observations. Climate Change: The IPCC Scientific Assessment (Wigley, TML, Barnett, TP), 239-256.

IPCC, 1992. Climate change 1992: the supplementary report to the IPCC scientific assessment (Houghton, J.T., Callander, B.A.). Cambridge Univ Pr.

Lal, R. (2003). Soil erosion and the global carbon budget.Environment International 29, 437- 450.

Maier, M., Schack-Kirchner, H., Hildebrand, E.E., Schindler, D., 2011. Soil CO2 efflux vs. soil respiration: Implications for flux models. Agricultural and Forest Meteorology 151, 1723-1730.

Maier, M., Schack-Kirchner, H., 2014. Using the gradient method to determine soil gas flux: A review. Agricultural and Forest Meteorology 192–193, 78-95.

Martin, J.G., Bolstad, P.V., 2009. Variation of soil respiration at three spatial scales: Components within measurements, intra-site variation and patterns on the landscape. Soil Biology and Biochemistry 41, 530-543.

Moldrup, P., Olesen, T., Schjønning, P., Yamaguchi, T., Rolston, D.E., 2000.Predicting the gas diffusion coefficient in undisturbed soil from soil water characteristics. Soil Science Society of America Journal 64, 94-100.

Mualem, Y., 1976. A new model for predicting the hydraulic conductivity of unsaturated porous media. Water Resources Research 12, 513-522.

Perrin, D., Laitat, É., Yernaux, M., Aubinet, M. 2004. Modélisation de la réponse des flux de respiration d'un sol forestier selon les principales variables climatiques= Modelling of the response of forest soil respiration fluxes to the main climatic variables. Biotechnologie, agronomie, société et environnement 8, 15-25.

Peters, W. et al., 2010. Seven years of recent European net terrestrial carbon dioxide exchange constrained by atmospheric observations. Global Change Biology 16, 1317-1337.

Pingintha, N., Leclerc, M.Y., Beasley, J.P., Zhang, G., Senthong, C., 2010. Assessment of the soil CO_2 gradient method for soil CO_2 efflux measurements: Comparison of six models in the calculation of the relative gas diffusion coefficient. Tellus, Series B: Chemical and Physical Meteorology 62, 47-58.

Quinton, J.N., Govers, G., Van Oost, K., Bardgett, R.D., 2010. The impact of agricultural soil erosion on biogeochemical cycling. Nature Geoscience 3, 311-314.

Reicosky, D.C., Lindstrom, M.J., Schumacher, T.E., Lobb, D.E., Malo, D.D., 2005. Tillage-induced CO2 loss across an eroded landscape. Soil and Tillage Research 81, 183-194.

Rommens, T., Verstraeten, G., Poesen, J., Govers, G., Van Rompaey, A., Peeters, I., Lang, A., 2005. Soil erosion and sediment deposition in the Belgian loess belt during the Holocene: Establishing a sediment budget for a small agricultural catchment. Holocene 15, 1032-1043.

Rumpel, C., Kögel-Knabner, I., 2011. Deep soil organic matter—a key but poorly understood component of terrestrial C cycle. Plant and Soil 338, 143-158.

Šimůnek, J., Suarez, D.L., 1993.Modeling of carbon dioxide transport and production in soil: 1. Model development. Water Resources Research 29, 487-497.

Smith, S.V., Sleezer, R.O., Renwick, W.H., Buddemeier, R.W., 2005. Fates of Eroded Soil Organic Carbon: Mississippi Basin Case Study. Ecological Applications 15, 1929- 1940.

Stallard, R.F., 1998. Terrestrial sedimentation and the carbon cycle: Coupling weathering and erosion to carbon burial. Global Biogeochemical Cycles 12, 231-257.

Tang, J.W., Baldocchi, D.D., Qi, Y., Xu, L.K., 2003. Assessing soil CO2 efflux using continuous measurements of CO2 profiles in soils with small solid-state sensors. Agricultural and Forest Meteorology 118, 207-220.

Takahashi, A., Hiyama, T., Takahashi, H.A., Fukushima, Y., 2004. Analytical estimation of the vertical distribution of CO2 production within soil: application to a Japanese temperate forest. Agricultural and Forest Meteorology 126, 223-235.

Topp, G.C., Davis, J.L., Annan, A.P., 1980. Electromagnetic determination of soil water content: Measurements in coaxial transmission lines. Water Resources Research 16, 574-582.

Tran, A. P., Bogaert, P., Wiaux, F., Vanclooster, M., Lambot, S., 2015. High-resolution space–time quantification of soil moisture along a hillslope using joint analysis of ground penetrating radar and frequency domain reflectometry data, Journal of Hydrology 523, 252–261.

Trumbore, S.E., Czimczik, C.I., 2008. Geology - An uncertain future for soil carbon. Science 321, 1455-1456.

Turcu, V.E., Jones, S.B., Or, D., 2005.Continuous soil carbon dioxide and oxygen measurements and estimation of gradient-based gaseous flux.Vadose Zone Journal 4, 1161- 1169.

Van Genuchten, M.T., 1980. A Closed-form Equation for Predicting the Hydraulic Conductivity of Unsaturated Soils1. Soil Sci. Soc. Am. J. 44, 892-898.

Van Oost, K., Verstraeten, G., Doetterl, S., Notebaert, B., Wiaux, F., Broothaerts, N., Six, J., 2012. Legacy of human-induced C erosion and burial on soil-atmosphere C exchange. Proceedings of the National Academy of Sciences of the United States of America 109, 19492-19497.

Wang, Z., Van Oost, K., Lang, A., Quine, T., Clymans, W., Merckx, R., Notebaert, B., Govers, G., 2014. The fate of buried organic carbon in colluvial soils: a long-term perspective. Biogeosciences 11, 873-883.

Webster, K.L., Creed, I.F., Beall, F.D., Bourbonnière, R.A., 2008a. Sensitivity of catchment-aggregated estimates of soil carbon dioxide efflux to topography under different climatic conditions. Journal of Geophysical Research G: Biogeosciences 113.

Webster, K.L., Creed, I.F., Bourbonniere, R.A., Beall, F.D., 2008b. Controls on the heterogeneity of soil respiration in a tolerant hardwood forest.Journal of Geophysical Research-Biogeosciences 113.

Wiaux, F., Cornelis, J.T., Cao, W., Vanclooster, M., Van Oost, K., 2014 a. Combined effect of geomorphic and pedogenic processes on the distribution of soil organic carbon quality along an eroding hillslope on loess soil. Geoderma 216, 36-47.

Wiaux, F., Vanclooster, M., Cornelis, J.T., Van Oost, K., 2014 b. Factors controlling soil organic carbon persistence along an eroding hillslope on the loess belt. Soil Biology and Biochemistry 77, 187-196.

Yoo, K., Amundson, R., Heimsath, A.M., Dietrich, W.E., 2005. Erosion of upland hillslope soil organic carbon: Coupling field measurements with a sediment transport model. Global Biogeochemical Cycles 19.

Young, S.L., Pierce, F.J., Streubel, J.D., Collins, H.P., 2009. Performance of solid-state sensors for continuous, real-time measurement of soil CO2 concentrations. Agronomy Journal 101, 1417-1420.

Tables

Table 1. Range of standard deviation and averaged values of triplicated measured hourly CO_2 concentrations at each depth, both at the summit and at the footslope position. This range is indicated by minimum (Min) and maximum (Max) values encountered along time (hourly time series) during the 6 months measurement period.

	Summit position				Footslope position			
Soil depth [cm]	Min mean [%]	Max mean [%]	Min S.D. [%]	Max S.D. [%]	Min mean [%]	Max mean [%]	Min S.D. [%]	Max S.D. [%]
10	0.07	1.39	0.00	0.71	0.26	4.75	0.00	3.13
25	0.06	1.83	0.00	0.68	0.30	3.93	0.00	5.32
45	NI	NI	NI	NI	0.12	3.96	0.00	1.96
95	0.15	2.83	0.00	1.42	0.48	7.52	0.00	2.48

Figures

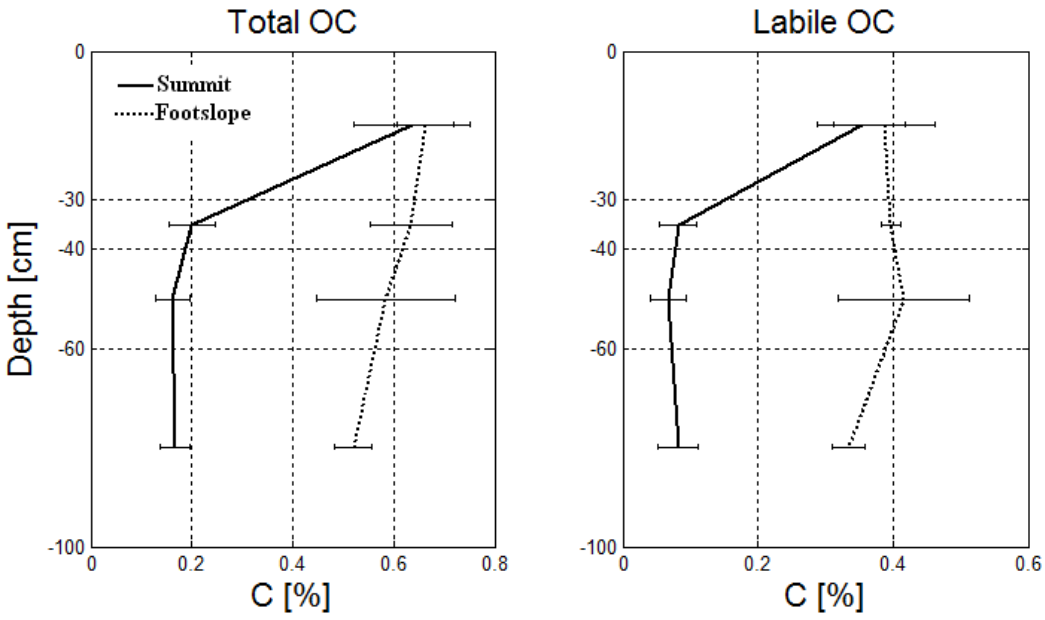

Fig. 1.Soil profiles (0-100 cm) of both soil total OC and labile OC pool concentrations [C%], at the summit and footslope positions. Error bars indicate 1 standard deviation (n≥3).

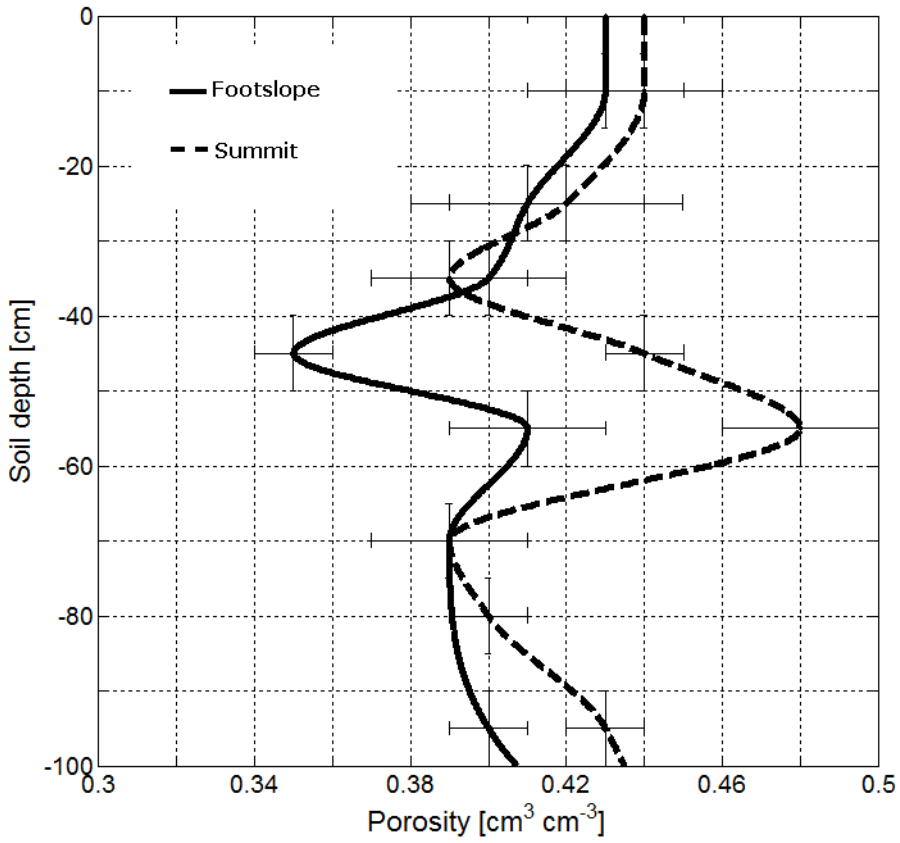

Fig. 2. Soil porosity profiles at the footslope (plain line) and at the summit (dashed line) positions. Error bars indicate 1 standard deviation (n≥3). Continuous lines are linearly interpolated values.

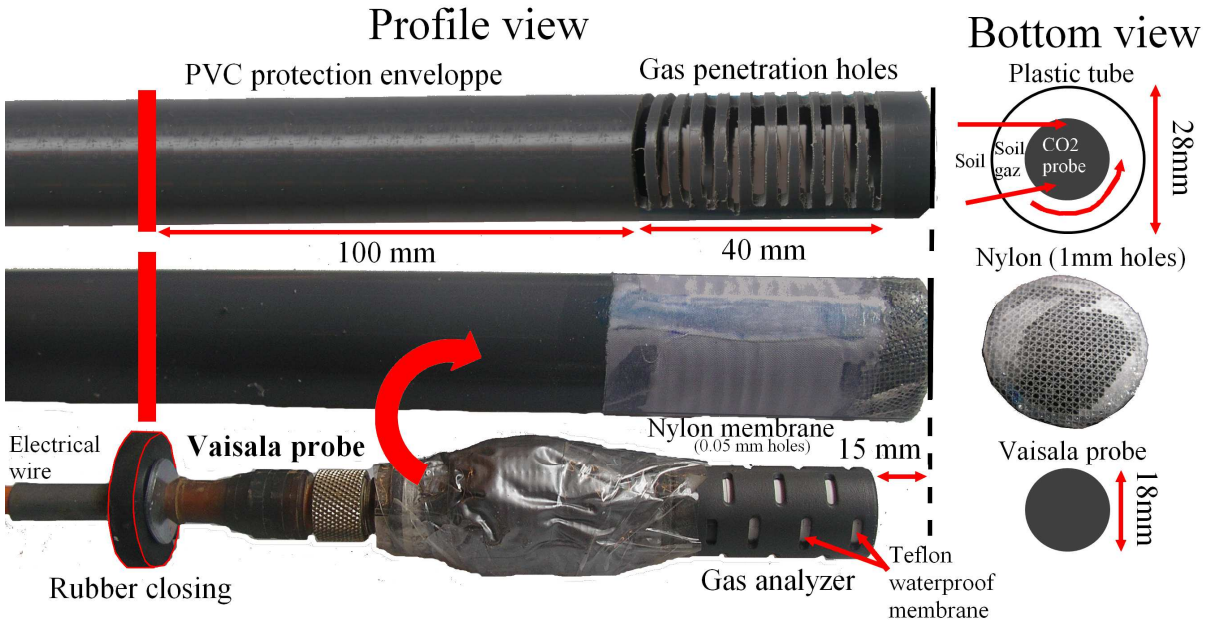

542

543 **Fig. 3. Description of the probes used for CO2 concentration measurements inside the soil.**

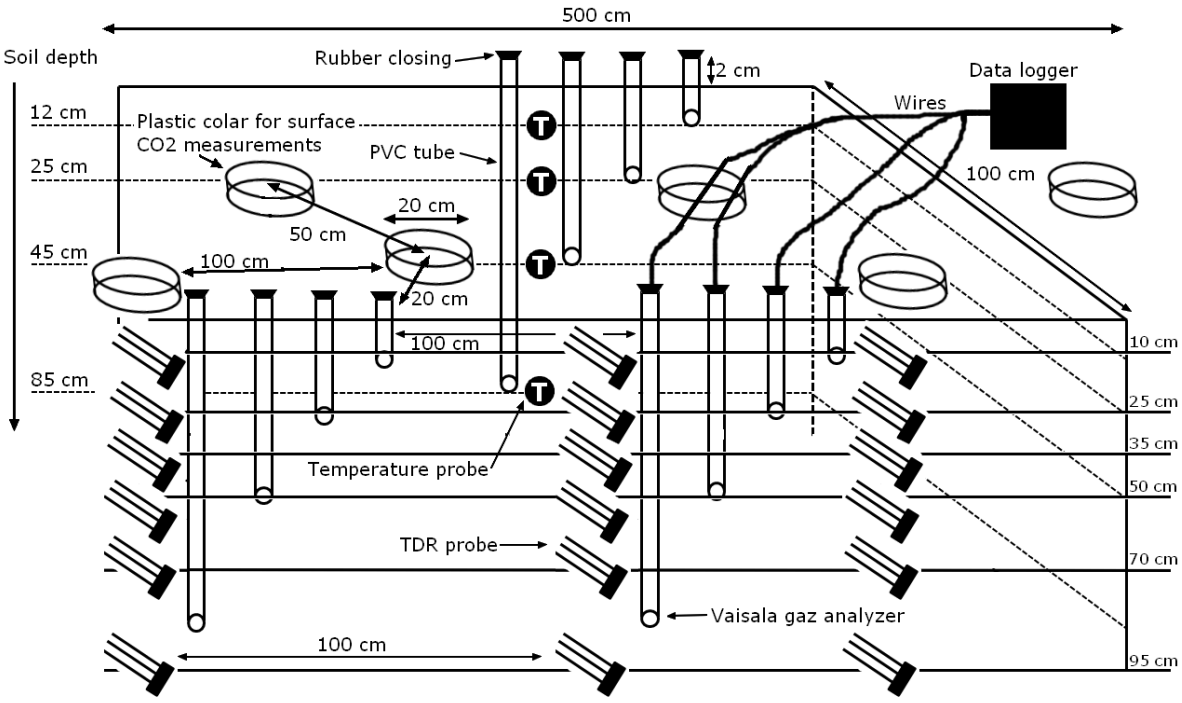

544

545 **Fig. 4. Schematic description of the experimental plot (sampling design) at each slope position showing how**
546 **temperature, VWC, CO_2 concentrations and CO_2 fluxes probes collocate with each others. Probes have been inserted**
547 **at different locations both vertically and horizontally. Consequently, all of them are not in the same plane (i.e. depth**
548 **lines with axes labels on the right hand-side illustrate the foreground profile and depth lines with axes labels on the**
549 **left hand-side illustrate the background profile).**

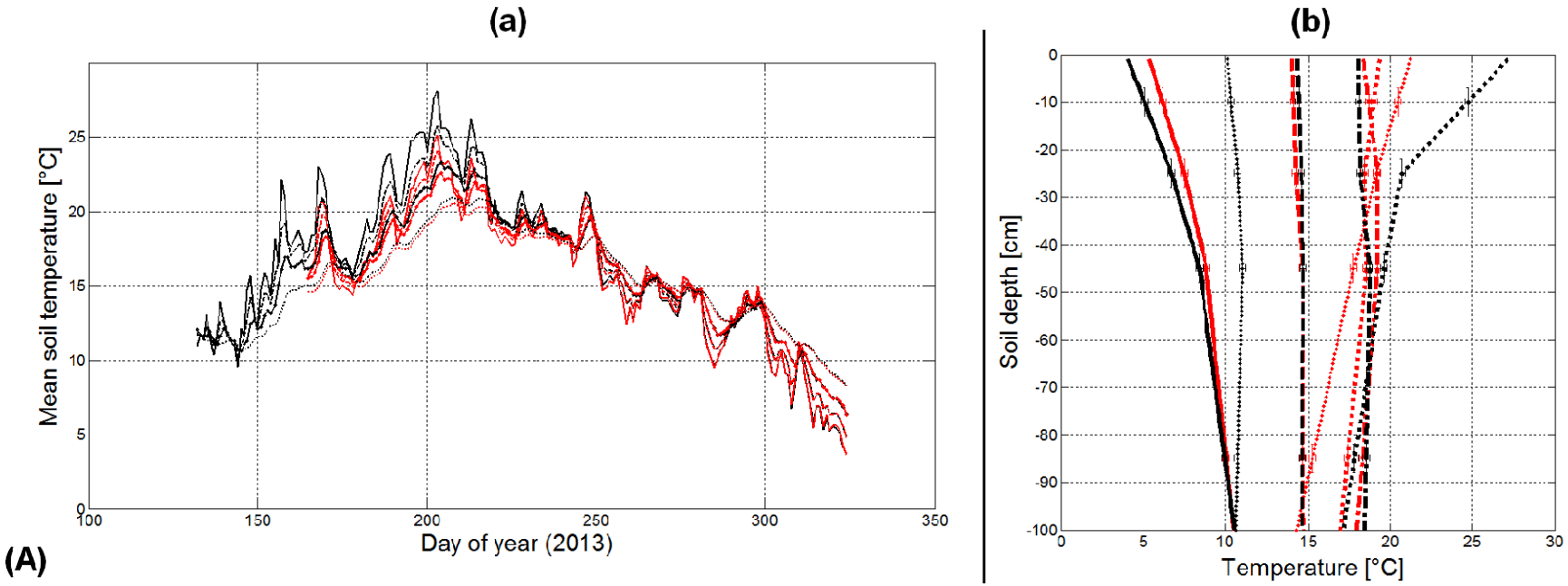
(a)
Mean soil temperature [°C]
Day of year (2013)
(b)
Soil depth [cm]
Temperature [°C]
(A)

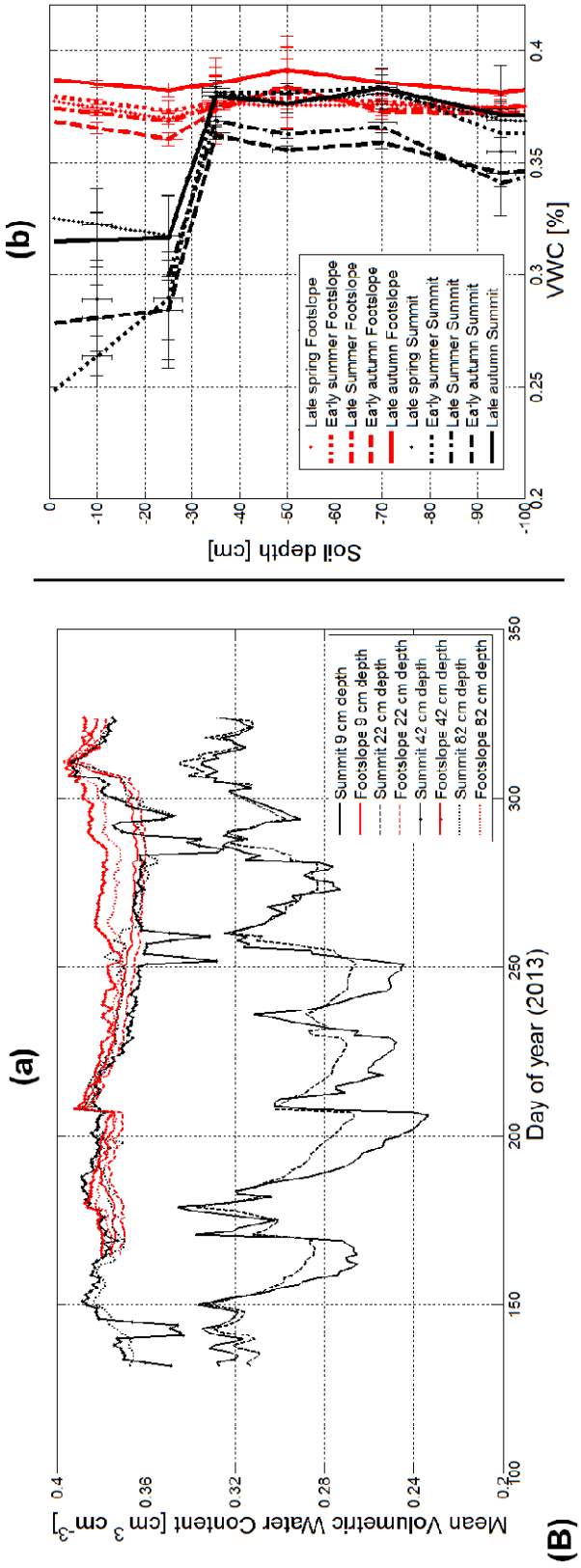

Fig. 5. Space-time dynamic of soil temperature (A) and moisture (B) at the summit (red) and the footslope (black) position in 2013: (a) time series at different depths; (b) Profile at different dates.

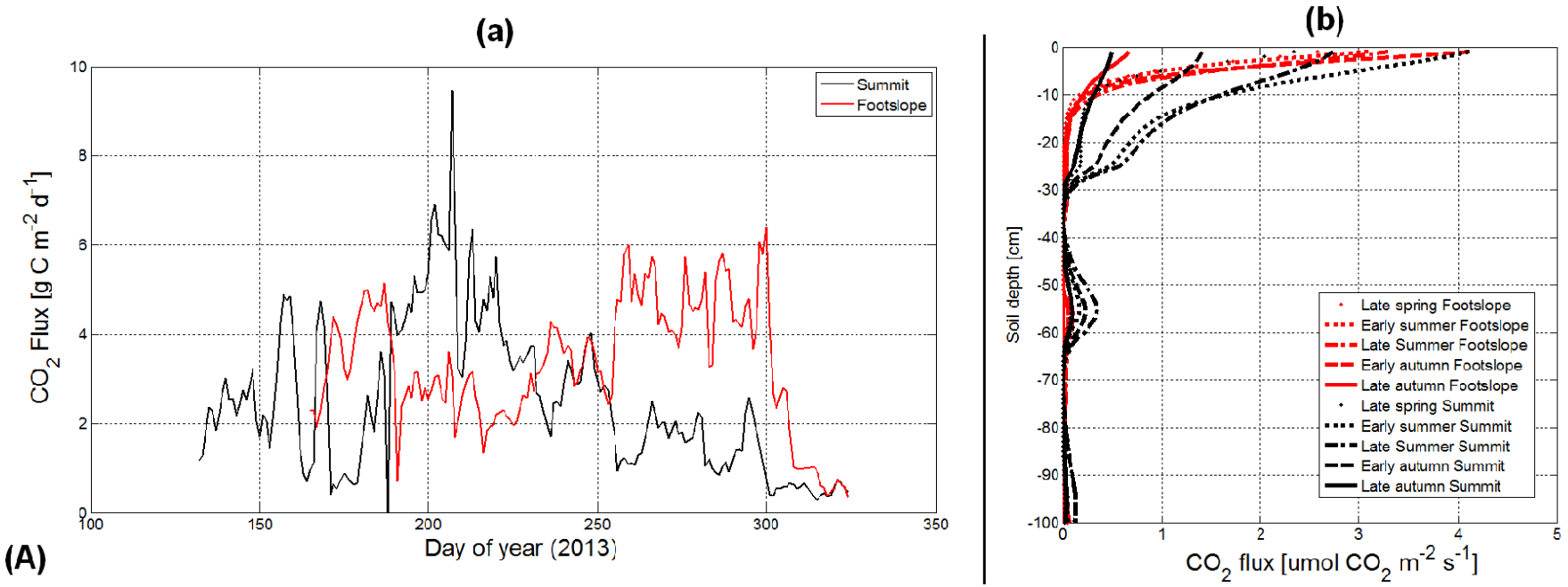
(a)
Summit
Footslope
CO_2 Flux [g C m^{-2} d^{-1}]
Day of year (2013)
(b)
Soil depth [cm]
CO_2 flux [umol CO_2 m^{-2} s^{-1}]
Late spring Footslope
Early summer Footslope
Late Summer Footslope
Early autumn Footslope
Late autumn Footslope
Late spring Summit
Early summer Summit
Late Summer Summit
Early autumn Summit
Late autumn Summit

(A)

555

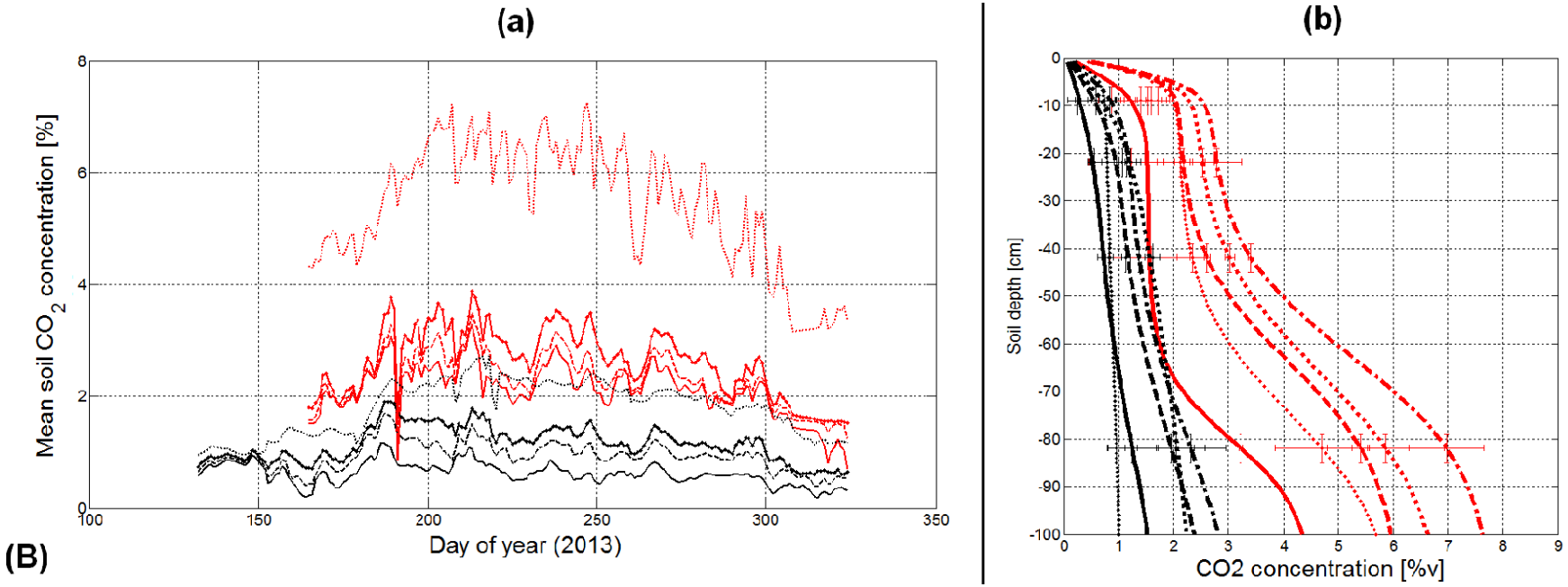
(a)
Mean soil CO_2 concentration [%]
Day of year (2013)
(b)
Soil depth [cm]
CO2 concentration [%v]

(B)

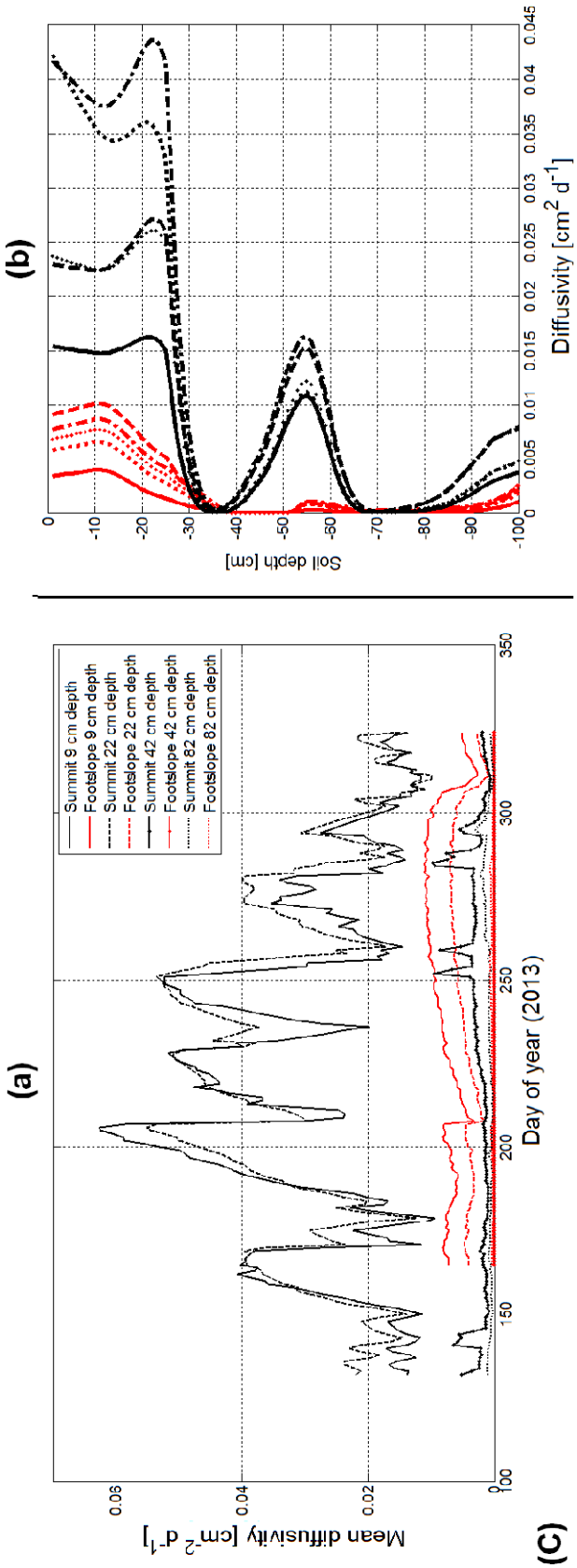

Fig. 6. Space-time dynamic of soil CO_2 fluxes (A) concentrations (B) and diffusivity (C), at the summit (red) and the footslope (black) position in 2013: (a) time series at different depths; (b) Profile at different dates.

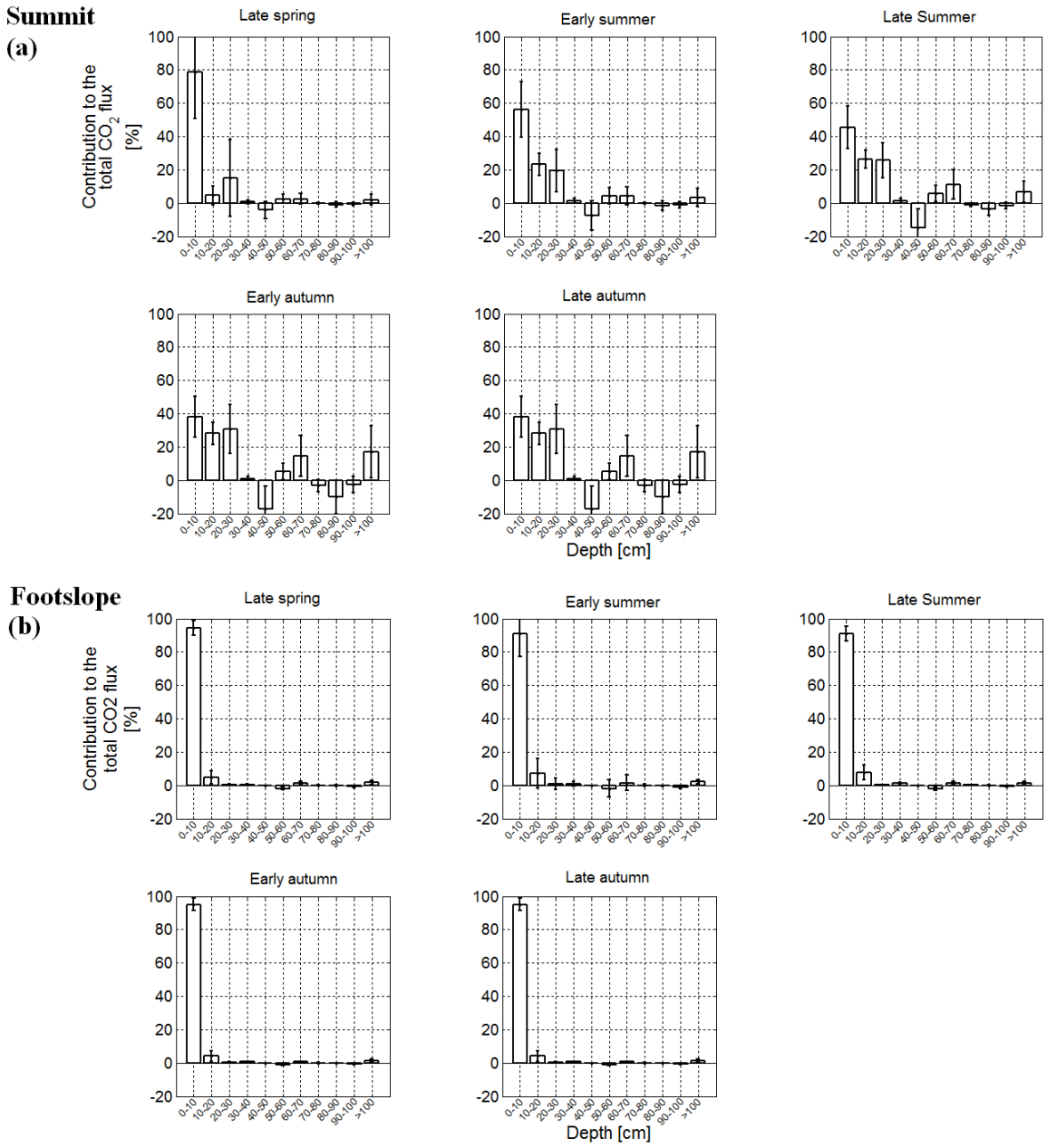

559

560 **Fig. 7. Depth distribution of the relative contribution to soilsurface CO_2 fluxes in year 2013 averaged by semi-seasons**
561 **(error bars represent the standard deviation of the time aggregation for each soil layer): (a) at the summit, and (b) at**
562 **the footslope position.**

563